Supplemental Data

Supplemental Note: Case Reports

Family 1 is from the United Arab Emirates (UAE), with 9 affected individuals in two branches, matching a recessive mode of inheritance. In this family, two brothers married two sisters that were both first cousins. All affected family members had normal pregnancy, labor, delivery, unremarkable newborn periods, and displayed typical developmental milestones. All affected individuals developed seizures between the ages of 1-2 years of age. The diagnosis of epilepsy predated developmental stagnation and loss of milestones. In some children, the presentation was consistent with sudden unexplained death in epilepsy (SUDEP, MIM: 617116). The connection with SUDEP was intriguing, and not well medically documented, but parents of both branches report that four of the children were healthy, then found dead during routine activities such as eating cereal, playing on a swing-set, or sleeping. The clinical presentation of this family did not match any reported conditions in the medical literature, and the physicians were not able to abate the clinical features with medical therapy.

Individual II-IV-6 was born full-term without complications. At 13 months, following a typical upper respiratory infection, he developed brief, absence-like episodes, which persisted weekly thereafter, mostly upon waking and without loss of consciousness. At 14 months he developed episodes that began with sudden stiffening of the back, followed by head deviation and loss of consciousness. These occurred 1-3 times per day, were diagnosed as generalized tonic-clonic seizures, and were refractory to antiepileptic treatment. At age 2 years, he showed signs of speech and developmental delay. MRI of the brain showed possible periventricular white matter loss but was otherwise structurally normal. EEG, EKG, karyotype, serum amino acids, lactate, pyruvate, and urine organic acids to evaluate for mitochondrial dysfunction were normal

repeatedly. At age 5 years, he was able to walk but his gait was unsteady and he suffered relapsing-remitting upper respiratory infection-associated cyclic episodes of depressed consciousness and hypoventilation requiring intubation, which each time was associated with further loss of developmental milestones. Muscle and nerve biopsies showed profound Type II fiber atrophy with severe axonal loss. The subject could not wean from the ventilator, requiring a tracheostomy and gastrostomy tube for life support. Following the resolution of an acute illness with supportive therapy, the his condition improved slowly and some previous skills returned, but this was quickly followed by further illness and loss of milestones. He had a series of cardiac arrests during acute exacerbations, but recovered with aggressive resuscitation. At age 9 years, MRI showed cerebral volume loss, amygdala and hippocampal atrophy (Fig. 1B). MR spectroscopy showed elevated N-acetyl aspartate in white matter voxels, suggesting ongoing neuronal degeneration. EEG showed frontal intermittent rhythmic delta activity and lack of clear posterior dominant rhythm, supporting white matter involvement. He did not improve significantly with physiotherapy and after a prolonged medically related transcontinental air flight, he died of respiratory failure at age 9. The clinical course for his sibling (II-IV-7) was similar to the index case except that she, with previously normal hearing, developed severe sensorineural hearing loss and paralysis of the right diaphragm during the course of her disease. MRI of the brain also showed possible periventricular white matter loss and enlarged ventricles, but was otherwise structurally normal. Repeated mitochondrial studies revealed no accumulation of relevant intermediates, and she remains in stable condition.

Family 2 is from Sicily with one affected individual, who is currently 16 years old. This boy is the second of two children born from healthy Sicilian parents, who report no consanguinuity (but are from the same village) and who have no history of neurological disorders. His growth parameters at birth were within normal range and the parents

report no concerns in the neonatal or early infantile age. Since the age of 10 years, he began experiencing balance difficulties and by age 11, showed gait abnormalities with progressive ataxia. Also at that time, abnormal ophthalmological features including nystagmus diplopia were noticed. His speech development was normal; however, his intellectual ability began to decline. At age 11, visually evoked potentials showed irregular waveform and amplitude within low limits. At the same time, the boy started to present cognitive difficulties and behavior abnormalities.

As part of the diagnostic work-up to define his condition, extensive metabolic and genetic investigations (including ataxia genes panel sequencing) were performed and fully reported as normal. Brain MRI performed at the age of 11 years showed cerebellar vermis hypoplasia/atrophy. There were some non-specific myopathic changes on his muscle biopsy. Peripheral nerve conductions studies showed low compound muscle action potentials (CMAPs) and axonal neuropathy. He developed ophthalmological features including nystagmus and diplopia. He also has severe scoliosis. Since the age of 10 years, he started to experience balance difficulties and since the age of 11, showed gait abnormalities with progressive ataxia. At the age of 14 years, there was a worsening of ataxia with severe difficulties in walking autonomously. He developed gynecomastia at the age of 10 years and endocrinological tests showed mild hypogonadism with elevated FSH values. Additionally, during the disease course, he experienced several episodes of hyperthermia, not responsive to paracetamol treatment, especially during the summer season. On last neurological examination at age of 15 years deep tendon reflexes were reduced. Cerebellar tests were impaired and he showed dysmetria. Tongue fasciculations were also noticed.

As part of the diagnostic work-up to define his condition, extensive metabolic and genetic investigations were performed without any pathological results. Brain MRI at age 11 showed cerebellar vermis hypoplasia/atrophy. There were some non-specific

myopathic changes on muscle biopsy. Peripheral nerve conductions studies showed low CMAPs and axonal neuropathy.

Family 3 is a Turkish family with one affected child born to consanguineous parents. She had normal developmental milestones. At the age of 4 years, she began to develop weakness in her upper and lower extremities and had difficulties in walking and abnormal gait. Cognitive functions remained initially normal. Her older brother had been diagnosed with cerebral palsy and died at the age of 9 years but further investigations have not been performed. Examinations at the age 8 years in another hospital revealed a mixed type polyneuropathy and sensorineural hearing loss, with normal brain and spine MRI. Since a chronic inflammatory polyneuropathy was suspected, an intravenous immunoglobulin treatment was started. However, there was no clinical benefit and she became wheelchair-dependent at the age of 12 years old.

Physical examination at the age of 12 years revealed symmetric muscle atrophy in upper and lower extremities. Muscle power was 4/5 and 3/5 in proximal and distal muscles of upper and lower extremities, respectively. There was thenar and hypothenar atrophy, claw hand and pes cavus deformities. Deep tendon reflexes were absent. Abduction of the eyes were restricted bilaterally. There were tongue fasciculations. Cerebellar tests were mildly impaired and speech was dysarthric. Brain MRI showed mild cerebellar atrophy. There were no dysmorphic features and mental functions were normal.

All metabolic investigations including serum and urinary amino acids, urinary organic acids, TANDEM analysis, very long chain fatty acids, serum biotidinase, serum ammonia, lactate and pyruvate were normal. Brain and spinal MRI showed mild cerebellar and spinal cord atrophy. On electroneuromyography, sensory responses were absent and only left median nerve could be stimulated. Nerve conduction of left median nerve was reduced (34.4 m/s) and amplitudes were very low (wrist: 390 µV and elbow:

328 μV). Needle electromyography showed polyphasic potentials. Repeated hearing test revealed moderate sensorineural hearing loss on the left and severe sensorineural hearing loss on the right.

Genetic analysis for *PMP22, SCA 1 and 2* were normal. Progressive hearing loss, axonal polyneuropathy and worsening of respiratory functions during infections suggested riboflavin responsive neuropathy, and co-enzyme Q10 (100 mg/day) and riboflavin (200 mg/day) were started. However, she did not benefit and weakness worsened. She became home-ventilator-dependent with tracheostomy. Mental function remained normal but she became bed ridden.

Family 4 originated from Pakistan, and parents were first cousins. Their first daughter was born after pregnancy complicated by gestational diabetes. Delivery and early development were normal. The subject was able to walk without support around age 18 months. She was diagnosed with asthma. At the age of two years, parents noted that gait became more unstable, with swaying of arms to keep her balance. During varicella infection, this deteriorated, and she was almost no longer able to sit and had a head tremor. Neurological examination at age 3.5 years showed mild dysarthria, a cerebellar eye movement disorder with saccadic pursuit and hypometric saccades, evident gait ataxia and mild intention tremor and dysmetria. In addition, muscle tendon reflexes were exaggerated at the legs, with bilateral Babinski signs. Funduscopy was normal. General pediatric exam was normal. MRI was initially normal. At the age of 4.5 years, she had mild cerebellar atrophy, which remained stable. Extensive metabolic investigations (plasma, urine and CSF) were normal except a slightly positive filipin test in fibroblasts, which led to the suspicion of Niemann-Pick type C disease. NPC1 and NPC2 were sequenced, but no explanation found. Muscle biopsy revealed non-specific mild atrophy of type 2 fibers and variation in fiber diameter; respiratory chain function in fresh tissue was normal as well as mitochondrial morphology. Whole-exome sequencing

in 2015 was initiated. Clinical course during the last 10 years remained remarkably stable (with the exception of deterioration with viral infections), and the subject was able to walk without support at age 13 years with mild mental retardation. Neurological examination showed spastic ataxia. Parents conveyed that high temperatures led to deterioration of symptoms. The youngest sister of the index individual was born after a pregnancy complicated by gestational diabetes, without complications. Early development was slow. She presented with generalized tonic-clonic seizures at age 9 months responding well to monotherapy with valproic acid. At age 2 years, she had mild global devlopmental delay, walked without support age at 18 months, spoke several words and some two-word combinations at age 23 months. Neurological examination at age 23 months was normal. Brain MRI as well as metabolic testing of plasma, urine and CSF was entirely normal, and whole-genome sequencing was initiated. This analysis revealed the same homozygous variant in *ADPRHL2* in both sisters, in addition to a *de novo* mutation in *CSNK2B*, c.T161A p.(Leu54Ter).

Family 5 was from Iran with 2 affected individuals, whose parents are first cousins. The proband (II-2) displayed normal developmental milestones until 18 months of age when she regressed significantly. She was noted to have muscle weakness and ataxic gaits. She began having epileptic attacks, which were controlled with phenobarbital; however, EEG and metabolic testing were normal. MRI performed at the age of 3 years showed abnormal white matter signal intensity in the bioccipital lobe but was otherwise structurally normal. EMG performed at the age of 3 years old indicated chronic sensorimotor distal polyneuropathy with axonal features. There were multiple oculomotor features including nystagmus, strabismus in one eye, putative external ophthalmoplegia with ptosis, impaired saccades, and upward gaze, suggesting brainstem dysfunction. She has recently started to walk with the help of her parents and she speaks only a few words and she has autistic features. Her affected brother (II-1)

exhibited similar presentation, with onset of symptoms around 18 months of age with frequent falling, hypotonia, muscle weakness, tremor and seizure controlled by valproate. Neurological examination at the age of 4 years showed that he was developmentally normal with normal cognition but the DTR are decreased. MRI taken at the age of 3 years old showed mild cerebellar atrophy. He was able to walk with difficulty. EMG and NCV at the age of 4 years old were normal. He also developed ataxia, poor balance and autistic features. He passed away at the age of 6 years old suddenly during sleep with no known cause.

Family 6 is a Turkish family with one affected female individual II-3 who is at the age of 16 years. She was born at term from healthy consanguineous parents after an uneventful pregnancy and delivery. She had two siblings. One of them died at the age of 18 years because of Wilson disease complications. The diagnosis of Wilson was confirmed pathologically. The other sibling was never able to walk independently and was first seen at the age of 11 months in another clinic because of motor delay and dropped head. His mental functions were normal but he developed severe scoliosis and distal muscle weakness and atrophy. He died suddenly due to SUDEP during the course of an upper respiratory tract infection.

Case II-3 was admitted to the neonatal intensive care unit for one week because of feeding difficulties and vomiting. She was later discharged and reached her motor milestones at normal ages. However, she had speech delay and started to talk at the age of 3 years. By the age of 13 years, she began to show gait abnormalities with difficulties in walking. She was admitted to a pediatric neurology clinic with the complaints of severe fatigue and progressive weakness.

On physical examination, she was in an apathic mood. Her upper extremity muscle strength was 4/5, lower extremity muscle strength was 3/5. Distal muscle groups were more affected than proximal muscle groups. She had symmetrical atrophy in

intrinsic hand and peroneal muscles. Deep tendon reflexes were increased and the Babinski sign was bilaterally positive. She also had a scoliosis and showed pes cavus deformities. Cerebellar examination revealed head titubation, mild intention tremor, head tremor and dysarthric speech. Her proprioception was also impaired and the Romberg sign with closed eyes was positive. WISC-R test performed at 15 years of age showed mild intellectual disability. The disease progressed to permanent muscular weakness of distal lower and upper extremities and she became wheelchair dependent at the age of 15.

Laboratory studies including complete blood cell count, infectious and metabolic evaluations revealed no abnormalities. Creatine kinase levels were slightly elevated ranging from 230 to 435 U/L (normal values: 0-145 U/L). Brain and spinal MRI performed at the age of 15 years showed mild cerebellar vermis atrophy and spinal cord atrophy. Ophthalmological examination, electroencephalography and auditory brainstem response (ABR) tests were normal. Nerve conduction studies revealed mild conduction delay in the right median nerve (40 m/sec) and the right tibial nerve (35 m/sec). Sural sensory responses could not be obtained. Peroneal nerves could not be stimulated. Compound muscle action potentials of right median and ulnar nerves were normal but compound muscle action potentials of tibial nerve were severely reduced (proximal: 330 µv, distal: 249 µv). Needle electromyography examinations at rest showed fibrillations and positive waves in tibialis anterior muscles consistent with severe denervation. Results were compatible with lower limb dominant axonal sensorimotor polyneuropathy.
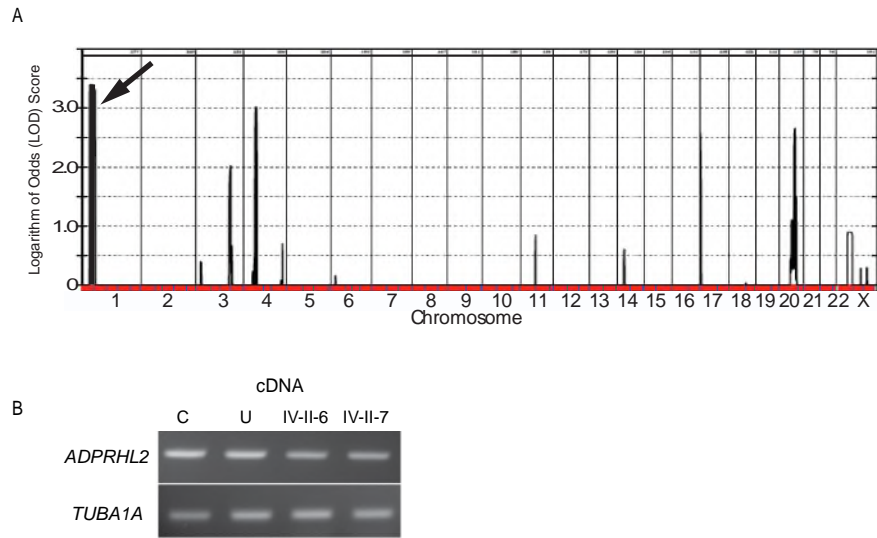
Figure S1. Linkage analysis and RT-PCR for family 1.
(A) Multipoint linkage plot for the family shows a peak on chromosome 1 with a maximum LOD score of 3.4 (arrow) and lower peaks on chromosomes 4 and 20. (B) RT-PCR results of fibroblasts from unrelated control (C), unaffected carrier Father (U), and affected individuals (IV-II-6 and IV-II-7) from Family 1 shows normal *ADPRHL2* mRNA t the

A

Family 3

	75	79	83

H. sapiens   Y T D D T A M A R
H. sapiens (mut)   Y T D D P A M A R

P. troglodytes   Y T D D T A M A R
M. mulatta   Y T D D T A M A R
M. musculus   Y T D D T A M T R
G. gallus   Y T D D T A M S R
D. rerio   Y S D D T A M M R
X. tropicalis   Y T D D T A M A R

Family 5

	173	177	181

H. sapiens   F A R L S A Q L T
H. sapiens (mut)   F A R L L A Q L T

P. troglodytes   F A R L S A Q L T
M. mulatta   F A R L S A Q L T
M. musculus   F A R L S A Q L T
G. gallus   F A K L S A E L T
D. rerio   Y S R F G A M L T
X. tropicalis   Y A R T S G M L T

Family 6

	30	34	38

H. sapiens   A L L G D C V G S
H. sapiens (mut)   A L L G N C V G S

P. troglodytes   A L L G D C V G S
M. mulatta   A L L G D C V G S
M. musculus   A L L G D C V G A
G. gallus   A L L G D C L G A
D. rerio   S V L G D C I G G
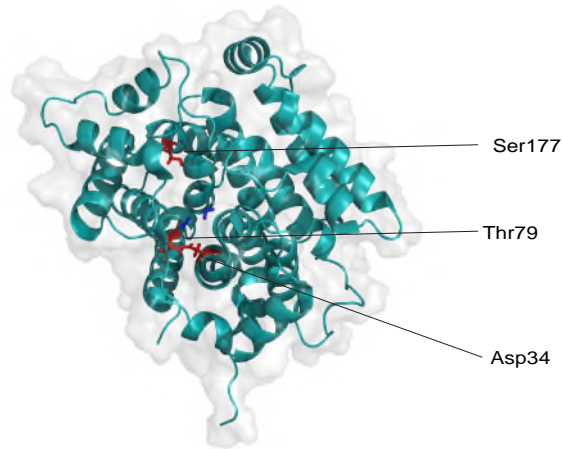X. tropicalis   A L L G D C I G A

B

Ser177

Thr79

Asp34

Figure S2. Families 3 and 5 carry *ADPRHL2* missense mutations that affect conserved amino acid residues.
(A) The amino acid missense mutations in Families 3, 5, and 6 are conserved in almost all vertebrates. (B) Cartoon model of *ADPRHL2* as solved at 1.6 Angstrom resolution [7]. Depicted are the mutated residues, Ser177, Thr79, and Asp34 in red within alpha-helical domains. Mg^{2+} ions are shown in blue.
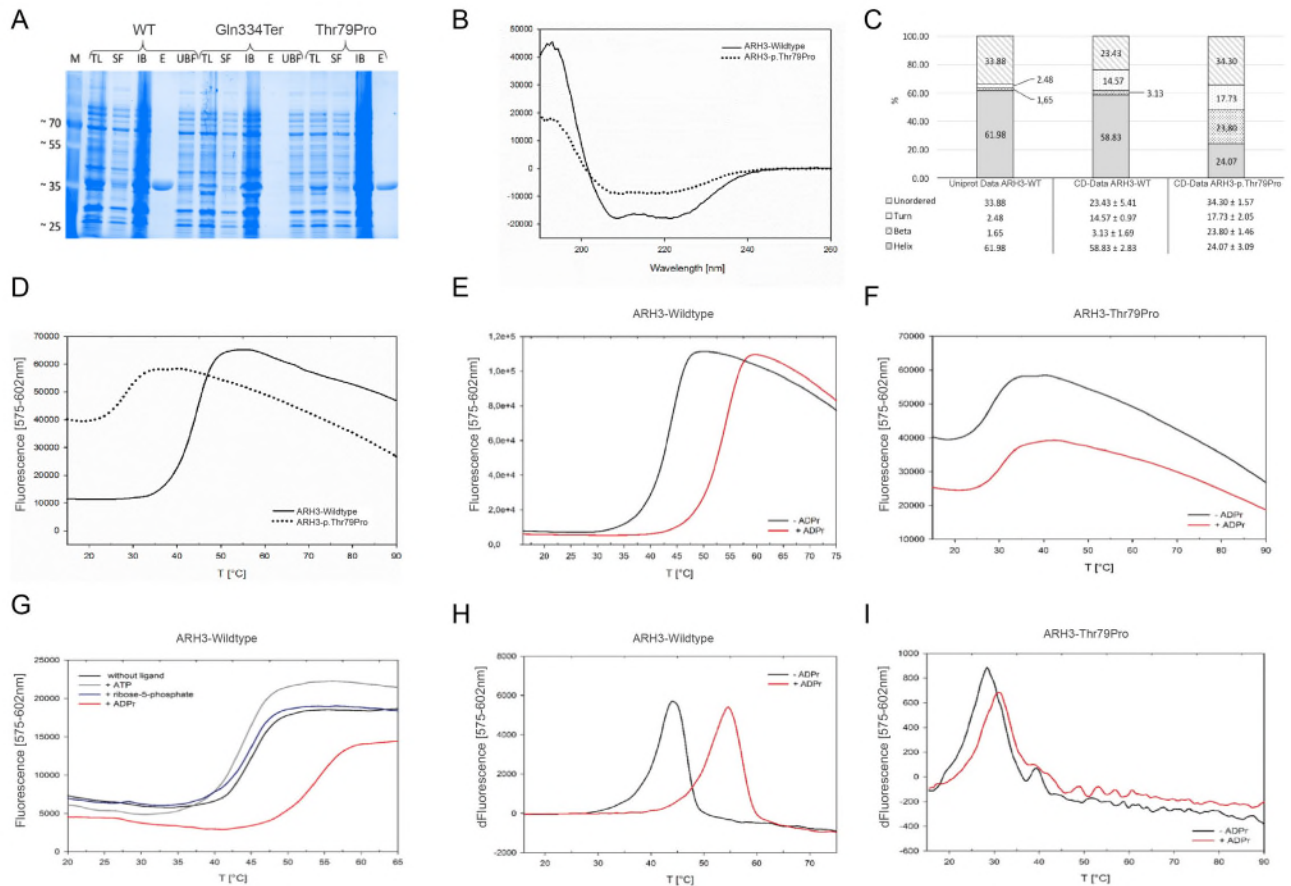
Figure S3. Biochemical characterization of Wildtype ARH3 and mutants on protein stability and substrate binding.

(A) Recombinant protein purification of ARH3 Wildtype (WT) and mutants with His-tag affinity chromatography. TL: total lysate, SF: soluble fraction, IB: inclusion body, E: elution of pure proteins, UBF: unbound flow through. (B-C) CD-spectroscopy measurement of secondary structure of ARH3-Wildtype and mutants. (B) Normalized exemplary presentation of the CD-spectra of recombinant ARH3-Wildtype and ARH3-p.Thr79Pro. Molar ellipticity [θ] measured at 10 °C in a range of 190-260 nm. (C) Experimentally determined composition of the secondary structural elements of ARH3-Wildtype and ARH3-p.Thr79Pro. Comparison of Uniprot data and CD-derived data from ARH3-Wildtype and ARH3-p.Thr79Pro. The data analysis was carried out with DichroWeb and is based on the algorithm CONTINLL [10,11]. The mean values and standard deviation of the CD-data analysis are tabulated in percent. ARH3-Wildtype n=3 NRMSD >0.05; ARH3-p.T79P n=3 NRMSD >0.08. (NRMSD= Normalized root-mean-square deviation). (D-I) Thermal stabilities of ARH3-Wildtype and ARH3-Thr79Pro measured via the thermofluor assay. Measured using 6 µg protein, ROX filter (575-602nm) and SYPRO orange dye. (D) Thermofluor melt curves of recombinant ARH3-

Wildtype and ARH3-p.Thr79Pro. Average melting temperatures: ARH3-Wildtype= 44.79 °C; ARH3-p.Thr79Pro= 28.37 °C. (E) Thermofluor melt curves of recombinant ARH3-Wildtype with different ligands (100 µM). Average melting temperatures: ARH3-Wildtype= 45.74 °C; ARH3-Wildtype+ ATP=44.57 °C; ARH3-Wildtype+ribose-5-phosphate=45.75 °C; ARH3-Wildtype+ADPr= 54.52°C. (F) Normalized and (G) derivative ARH3-Wildtype melt curve in the presence of adenosine diphosphate ribose (ADPr). Average melting temperatures: ARH3-Wildtype= 43.87 °C; ARH3-Wildtype+ADPr= 54.59 °C. (H) Normalized and (I) derivative ARH3-p.Thr79Pro melt curve. Average melting temperatures: ARH3-p.Thr79Pro= 28.37 °C; ARH3-p.Thr79Pro + ADPr= 31.05 °C.
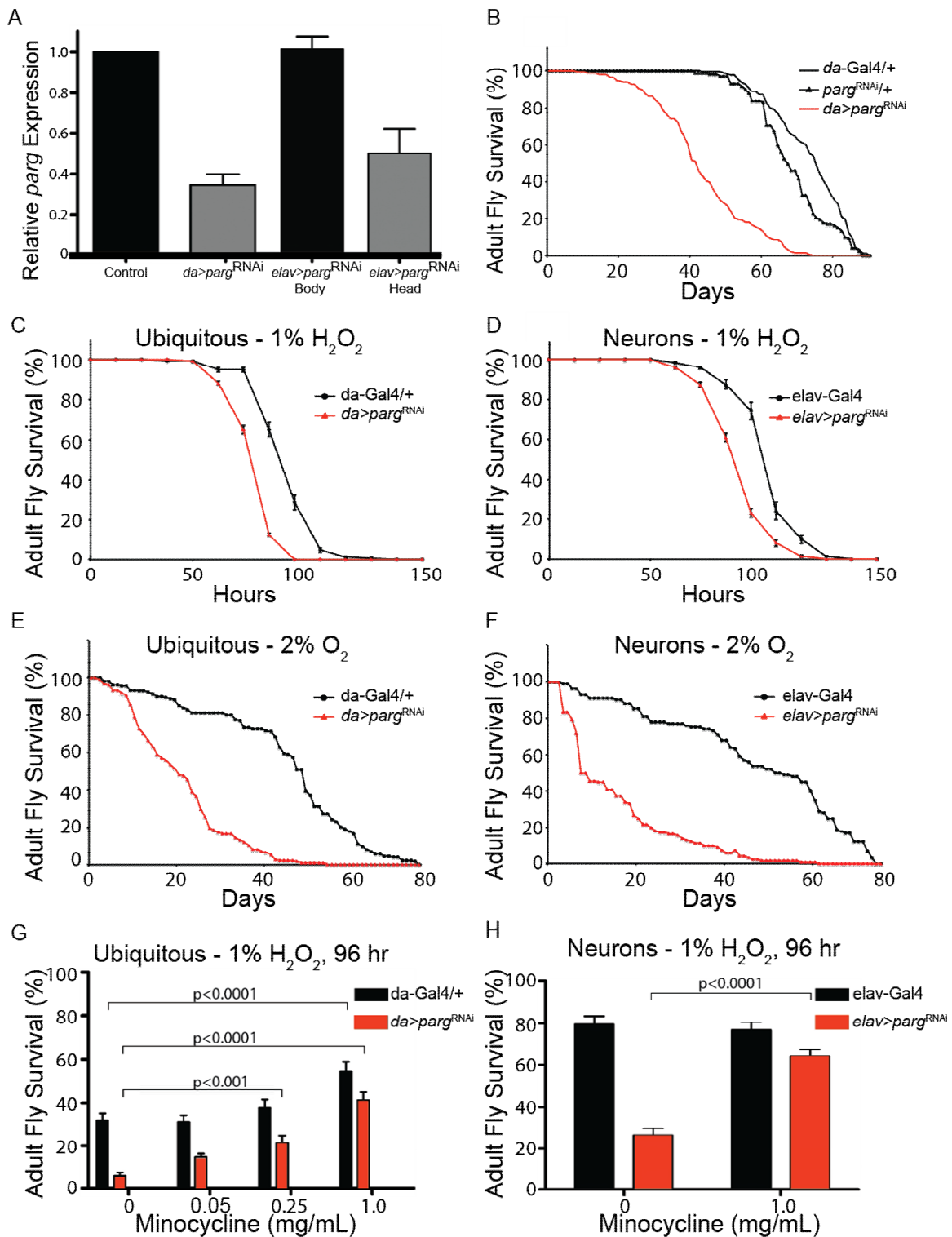
Figure S4. *Drosophila mutants* **display increased survival with PARP inhibition.**
(A) Relative *parg* expression in ubiquitous knockdown animals under the *daughterless (da)* promoter shows that RNAi leads to an ~60% in *parg* mRNA levels. Relative *parg*

expression in neuron-specific knockdown animals under the *elav* promoter shows that RNAi leads to an ~50% in *parg* mRNA levels in the head of the animal only.(B) Mutant flies with a ubiquitous decrease in *parg* by RNAi die prematurely (red) compared with parental stocks (black). (C,E) Flies with ubiquitous knockdown of *parg* under the *daughterless (da)* promoter display decreased survival when exposed to oxidative stress or low oxygen. (D,F) Flies with knockdown of *parg* under the neural *elav* promoter display decreased survival when exposed to oxidative stress or low oxygen. (G,H) Flies with ubiquitous and neuronal knockdown of *parg* can show increased survival in the presence of hydrogen peroxide when pre-treated with Minocycline. Kaplan–Meier Log-rank Test. Data is mean ± s.e.m. of n=8 experiments.

Supplemental Tables

Family	Gene	Transcript	gDNA pos.	cDNA pos.	Protein pos.
Family 1	*ADPRHL2*	NM_017825.2	g.36558895C>T	C.1000C>T	p.Gln334Ter
Family 2	*ADPRHL2*	NM_017825.2	g.36557226C>T	c.316C>T	p.Gln106Ter
Family 3	*ADPRHL2*	NM_017825.2	g.36556868A>C	c.235A>C	p.Thr79Pro
Family 4	*ADPRHL2*	NM_017825.2	g.36557324_36557328delTGCCC	c.414_418delTGCCC	p.Ala139Glyfs*4
Family 5	*ADPRHL2*	NM_017825.2	g.36557524C>T	c.530C>T	p.Ser177Leu
Family 6	*ADPRHL2*	NM_017825.2	g. 36554605G>A	c.100G>A	p.Asp34Asn

Table S1. Detailed information for all mutations detected in affected individuals from families 1-6, including gene name, transcript number, genetic (gDNA) and complementary DNA (cDNA) position, and protein position.

Materials and Methods

Linkage Analysis and Exome Sequencing

This study was approved by the Institutional Review Board at the respective host institutions. All study participants signed informed consent documents, and the study was performed in accordance with Health Insurance Portability and Accountability Act (HIPAA) Privacy Rules. DNA was extracted from peripheral blood leukocytes with salt extraction and genotyped with the Illumina Linkage IVb mapping panel [1]. LOD scores were calculated using easyLinkage-Plus software [2] using genotype results of all consenting family members in the parental and affected generations. Fine mapping of selected individuals was performed using the Affymetrix 250K Nsp1 SNP array and results analyzed using identity-by-descent mapping. Exome capture was performed using the Agilent SureSelect Human All Exome 50Mb Kit and paired-end sequenced on an Illumina instrument [3]. Depth of coverage was 30±16 (s.d) per exome and exome data was analyzed as previously described [4]. Whole exome sequencing for case II-1 family 3 was performed on on an Illumina Hiseq 4000, using the SureSelect Human All Exon V6 enrichment kit and a paired-end 75bp sequencing protocol and data analysis and filtering for autosomal recessive inheritance was performed as previously described [5].

Whole genome sequencing (WGS)

For case II-3 from family 6, the DNA libraries for Trio-Whole Genome Sequencing were prepared for WGS using Illumina´s TruSeq PCR-Free sample preparation kit according to manufacturer instructions. In short, 1 μg of gDNA was fragmented to a mean target size of 350-450 bp using a Covaris E220 instrument, followed by end-repair, 3'-adenylation and ligation of indexed sequencing adaptors. The quality and concentration of all sequencing libraries was assessed using a LabChip GX instrument (Perkin Elmer),

followed by further quality control using a MiSeq sequencer (Illumina) to obtain optimal cluster densities, insert size and library diversities. Sequencing libraries (one sample per lane) were hybridized to the surface of HiSeqX flowcells (v2 or v2.5) using the Illumina cBot™. Paired-end sequencing-by-synthesis (SBS) was performed on Illumina HiSeqX sequencers, using 2x150 cycles of incorporation and imaging. Real-time analysis involved conversion of image data to base-calling in real-time. All steps in the sample preparation and sequencing workflow were monitored using an in-house laboratory information management system (LIMS) with barcode tracking of all samples and reagents. The GRCh37 reference sequence was used to map reads. The raw sequences were aligned to reference sequence using BWA version 0.7.10. The sequences in the BAM files were realigned around indels with GATKLite version 2.3.9 using a public set of known indels. PCR duplicates marked with Picard tool version 1.117. We filtered out the variants with low map quality, low read depth (<6x), low Phred-scaled SNP quality score (<20) and strong strand bias. Variants were analyzed using the Clinical Sequence Miner application (DeCODE Genetics, Iceland). Low-quality variants, variants with call ratios of less than 20%, and variants with global allele frequencies higher than 0.01 were excluded from analysis according to Exome Aggregation Consortium (ExAC), Genome Aggregation Database (GnomAD) and Greater Middle East Variome project (GME Variome). Variants were analyzed under the assumption of being present or homozygous in the affected individual and absent or heterozygous in the unaffected parents. Variants were prioritized according to *in silico* pathogenicity score using Phred-scaled score provided by Combined Annotation Dependent Depletion (CADD).

Both affected siblings from family 4 underwent whole genome sequencing. In brief, Sample prep (TruSeq DNA, input 250 ng) and the Illumina's HiSeqX sequencing platform were used according to manufacturer's instructions to perform WGS with

2x150bp read length. Illumina data were processed with the inhouse developed pipeline (https://github.com/hartwigmedical/pipeline), with settings validated for clinical genetics version 1.12 (https://github.com/hartwigmedical/pipeline/blob/master/settings/KG.ini). The 20x coverage of the exome target sequence was >95% for all samples. Variants present in the protein coding region or those that potentially affect splicing, +/- 6 base pairs into the intron, were prioritized using Cartagenia Bench Lab NGS (Agilent Technologies, Santa Clara, USA) based on population allele frequency and anticipated inheritance patterns. Further interpretation was performed based on predicted functional impact of the variants and literature.

Reverse Transcription (RT) PCR

Fibroblasts from affected individuals were harvested from punch biopsy and grown as previously described [6]. For the relative quantification of mRNA expression, total RNA from quantified subject and control fibroblasts was reverse-transcribed using the Superscript III First-Strand cDNA Kit (Invitrogen). PCR analysis of cDNA was performed using dHPLC-purified primers designed against exons 4-6 of *ADPRHL2* excluding introns and PCR products were visualized using standard techniques.

Antibodies

ADPRHL2 (Sigma HPA027104); Tubulin (Sigma T6074).

Western Blot

Patient and healthy control fibroblasts were grown to 90% confluence, pelleted, and lysed in the treatment buffer (20mM Tris-HCl pH 8, 137mM NaCl, 1% Triton X-100, 2mM EDTA) with a cocktail of protease inhibitors (Complete Protease Inhibitor Cocktail Tablets, Roche). Protein quantification was performed with the BCA Protein Assay Kit

(Pierce), 25 µg of the protein samples were run on standard 10% SDS-PAGE gels, and transferred to a PVDF membrane. Membranes were then blocked in either 5% non-fat milk powder or 4% BSA in Tris-buffered saline Tween (TBST), incubated overnight in the primary antibody solutions, washed, and incubated in the HRP-conjugated secondary antibody solutions for 1 hour. Bands were visualized using an appropriate chemilluminescence detection reagent.

Protein Purification

Wildtype *ADPRHL2* cDNA was cloned into pET15b vector and mutations were introduced via mutagenesis with NEB Q5 mutagenesis kit. Recombinant proteins were purified with *Escherichia coli BL21-CodonPlus (DE3)-RIPL* competent cells (Agilent) according to previous study [7].

Thermofluor Assay

6 µg of purified protein was re-buffered in Hepes buffer (10 mM Hepes; 1 mM MgCl$_2$; 5 % Glycerol; pH 7.0) and mixed with 10 x SYPRO™ Orange Protein Gel Stain in DMSO (Invitrogen™) to a total volume of 25 µl. 100 µM ligands (adenosine diphosphate ribose (ADPr); adenosine triphosphate (ATP); ribose-1-phosphat (r-1-P); ribose-5-phosphat (r-5-P)) were added to test their influence on the thermal stability. Triplicates were pipette in a 96 well plate, heated up to different temperatures in a rage of 15-70 °C and measured the fluorescence with Applied Biosystems 7500 Real-Time PCR System, using the ROX filter. Data were analyzed with Protein Thermal Shift™ Software (Thermo Scientific™).

Circular Dichroism (CD) Spectroscopy

40-50 µg purified protein were re-buffered in NaPO4 (10 mM; pH 7.0) and diluted in a total volume of 200 µl. Proteins were heated from 10°C to 70°C in 5-10°C steps in the range of 180-260 nm or with variable temperature from 10-70 °C (1°C/minute) while measuring the θ mdeg with the Jasco J-715 CD-spectrometer at 221 nm. Data were

collected in cuvette with 1 mm path length and analyzed with DichroWeb using the CONTINLL algorithm and the reference set 7 (25; 26). Data were normalized for molarity to obtain the mean residual elipticity.

Drosophila **Stocks and Crosses**

UAS-Dicer 2 (#24650), daughterless (da)-Gal4 (#5460), and elav-Gal4 (#458) were obtained from the Bloomington Stock Center (Indiana). Parg[27.1] was kindly provided by A. Tulin as described [8]. UAS-PargRNAi (#23964GD) was obtained from VDRC (Vienna). All Gal4 and UAS strains were out-crossed into w1118 at least 6 times. Flies were maintained at room temperature. Experiments were performed at 25°C. Dicer-2 (Dcr) was included in RNAi experiments together with da>Gal4 or elav-Gal4 to enhance RNAi effects [9]. Homozygous elav-Gal4; UAS-Dcr and da-Gal4;UAS-Dcr stocks were established by standard genetic crosses, then crossed to either to UAS-Parg RNAi for RNA knock-down or to w1118 for control in respective experiments [9].

Quantitative PCR (qPCR)

Total RNA was isolated from whole flies, heads, or bodies using Trizol (Invitrogen) and the RNeasy Mini Kit (Qiagen) according to the manufacturer's instructions. cDNA synthesis was performed with oligo-dT and random primers using SuperScript III first-strand synthesis system (Invitrogen). qPCR was performed in duplicate using SYBR

Green on an ABI 7900HT qPCR system (Applied Biosystems) according to the manufacturer's protocol. All samples were analyzed from at least 3 independent experiments. Data was normalized to the level of rp49 mRNA prior to quantifying the relative levels of mRNA between controls and experimentally treated samples.

Oxidative Treatment

Four to five day-old males, grouped with 20 flies per vial, were fed on a 3mm Whatman paper soaked with 1% hydrogen peroxide (Sigma) in 5% sucrose/PBS. Control flies were fed 5% sucrose/PBS. Under this condition, flies live up for 10 days without consequence. Scores were generated every 12 hours for the number of dead flies. Fresh hydrogen peroxide was added daily. For Minocycline experiments, flies were fed first with 5% sucrose/PBS or 5% sucrose/PBS/Minocycline for 24 hours prior to adding hydrogen peroxide (n=160 flies per genotype for all experiments).

Hypoxic Treatment

Male flies were collected within 24 hours of eclosion, placed at a density of 20 flies per vial, and aged for 2-3 days before subject to hypoxia. Flies were fed with standard food, maintained in a hypoxic chamber (COY Laboratory Products INC) filled with 2% oxygen at 22°C, and transferred every 2 day to new vials within the chamber without exposure to air, therefore avoiding re-oxygenation. The number of dead flies was scored daily (n=200 flies per genotype).

Lifespan

Parg[27.1] and w1118 flies were allowed to produce eggs and develop until second instar larvae at 25°C. The larvae were then transferred to an incubator at 29°C until eclosion. Adult flies were collected within 24 hours of eclosion, grouped 10 males per vial on

standard fly food, and placed back at 25°C. Flies were passed every day and dead flies were scored until all Parg[27.1] flies were dead (n=60 Parg[27.1] and n=120 w1118 flies).

Statistical Analyses

Survival was analyzed by Kaplan–Meier Log-rank Test and Gene expression was analyzed by the Student's t-test or One-way ANOVA with Dunnett's post test using Graph Pad Prism4 software. $p < 0.05$ was considered statistically significant.

Supplemental References

1.   Murray, S.S, Oliphant, A., Shen, R., McBride, C., Steeke, R.J., Shannon, S.G., Rubano, T., Kermani, B.G., Fan, J.B., Chee, M.S., et al. (2004). A highly informative SNP linkage panel for human genetic studies. Nat Methods 1, 113-117.

2.   Hoffmann, K. & Lindner, T.H. (2005). easyLINKAGE-Plus--automated linkage analyses using large-scale SNP data. Bioinformatics 21, 3565-3567.

3.   Gnirke, A., Melnikov, A., Maguire, J., Rogov, P., LeProust, E.M., Brockman, W., Fennell, T., Giannoukos, G., Fisher, S., Russ, C., et al. (2009) Solution hybrid selection with ultra-long oligonucleotides for massively parallel targeted sequencing. Nat Biotechnol 27, 182-189.

4.   Dixon-Salazar, T.J., Silhavym J.L., Udpa, N., Schroth, J., Bielas, S., Schaffer, A.E., Olvera, J., Bafna, V., Zaki, M.S., Abdel-Salam, G.M., Mansour, L.A., et al (2012). Exome sequencing can improve diagnosis and alter patient management. Sci Transl Med 4, 138ra178.

5.   Alawbathani S., Kawalia, A., Karakaya, M., Altmuller, J., Nurnberg, P., Cirak, S. (2018). Late diagnosis of a truncating WISP3 mutation entails a severe phenotype of progressive pseudorheumatoid dysplasia. Cold Spring Harb Mol Case Stud 4, a002139.

6.   Villegas, J. & McPhaul, M. (2005). Establishment and culture of human skin fibroblasts. Curr Protoc Mol Biol Chapter 28, Unit 28 23.

7.   Mueller-Dieckmann, C, Kernstock, S., Lisurek, M., von Kries, J.P., Haag, F., Weiss, M.S., Koch-Nolte, F. (2006). The structure of human ADP-ribosylhydrolase 3 (ARH3) provides insights into the reversibility of protein ADP-ribosylation. Proc Natl Acad Sci USA 103, 15026-31.

8.   Hanai, S., Kanai, M., Ohashi, S., Okamoto, K., Yamada, M., Takahashi, H., Miwa, M. (2004). Loss of poly(ADP-ribose) glycohydrolase causes progressive neurodegeneration in Drosophila melanogaster. Proc Natl Acad Sci U S A 101, 82-86.

9.   Dietzl, G., Chen, D., Schnorrer, F., Su, K.C., Barinova, Y., Fellner, M., Gasser, B., Kinsey, K., Oppel, S., Scheiblauer, S., et al (2007). A genome-wide transgenic RNAi library for conditional gene inactivation in Drosophila. Nature 448, 151-156.

10.   Whitmore, L. and Wallace, B.A. (2004) DICHROWEB, an online server for protein secondary structure analyses from circular dichroism spectroscopic data. Nucleic Acids Res 32, W668-73.

11.   Sreerama, N. and Woody, R.W. (2000). Estimation of protein secondary structure from circular dichroism spectra: comparison of CONTIN, SELCON, and CDSSTR methods with an expanded reference set. Anal Biochem 287, 252-60.